Annu. Rev. Physiol. 1994. 56:213–36

Ca^{2+}-BINDING AND STRUCTURAL DYNAMICS IN THE FUNCTIONS OF CALMODULIN

Harel Weinstein and Ernest L. Mehler
Department of Physiology and Biophysics, Mount Sinai School of Medicine, City University of New York, New York, NY 10029–6574

KEY WORDS: cellular Ca^{2+}, calcium-binding proteins, cooperativity, protein structure, EF-hand motifs, hydrophobic patches, molecular modeling, molecular dynamics simulations

INTRODUCTION

The large number of recent reviews and evaluations devoted to the actions of calmodulin (CAM) as a mediator of Ca^{2+} signaling reflects the great interest in the key role of Ca^{2+} in a variety of processes in the cell (6, 19, 20, 26, 82), as well as the rapid increase in understanding the role of CAM in the mechanisms underlying these essential physiological functions (10, 21, 28, 33, 36, 56, 57, 59, 66, 83, 99, 100, 110, 117, 139). The examples discussed in these compendia characterize in detail some of the regulatory actions of calmodulin in the cell, but the list of such actions is growing with the continuing identification of specific targets for activation by CAM (e.g. see 6, 18, 29, 43, 53, 140). Recent explorations of CAM-regulated processes have taken advantage of the special physiological properties of a variety of organisms in which the direct requirements for Ca^{2+}-activated CAM can be revealed by genetic manipulation (25, 75). Such approaches exploit strain-specific variants of CAM (e.g. see 41, 66, 69, 76, 106), as well as differences in the properties of its targets [e.g. the CAM-regulated kinases (99) and the phosphatases that have been described earlier in vertebrates (8)]. The functional insights emerging from these studies, focused on the actions of Ca^{2+}-activated CAM, are gaining mechanistic value from

0066–4278/94/0315–0213$05.00

the inferences provided by rapidly accumulating data about the three-dimensional structural characteristics of the CAM molecule (e.g. see 5, 7, 15, 31, 46, 60, 85, 92, 97, 120) and its complexes with ligands (e.g. see 45, 47, 52, 61, 62, 77, 81). The literature summarizing the structural characteristics of CAM emphasizes those shared with other calcium-binding proteins (especially the EF-hand class; 80, 109), as well as those structural elements that appear to set CAM apart from other members of this family of proteins, and determine the specificity of its interaction with the various targets in the cell (7, 14, 31, 32, 47, 52, 53, 60–62, 77, 81, 85, 92, 94–96, 120, 128). Based on such structural data, hypotheses regarding the mechanisms of action of CAM in a variety of physiological processes can be formulated at a detailed molecular level (e.g. see 30, 87, 90–92, 94, 98, 99, 108, 126). Such hypotheses can serve to identify and discriminate the differences in the structural properties that underlie the diverse actions of CAM in the various physiological mechanisms it subserves in the cell. A practical consequence of the mechanistic insights at the molecular level is the opportunity they may offer to achieve specific control over the many processes that depend on Ca^{2+} concentration gradients and their decoding by CAM (e.g. see 9, 17, 96, 135). One promising avenue for achieving such control through structural manipulation is the application of protein engineering approaches to CAM based on a structurally-defined design strategy (138).

However, it is becoming increasingly clear that the CAM molecule has special dynamic properties that characterize its structure (7, 46, 47, 63, 85, 92, 128), determine the effects of Ca^{2+} binding on the biological properties of the molecule (e.g. see 31, 35, 55, 110, 119), and affect the interactions of CAM with its cellular targets (30, 32, 47, 52, 62, 77, 81, 100). These dynamic structural characteristics are major determinants of the capacity of CAM to carry out its actions in the cell with the significant functional selectivity and high fidelity required of an ubiquitous modulatory agent (e.g. see 56, 58, 66). Consequently, an essential requirement for understanding how CAM performs its diverse functions is information that reaches beyond the structural details, to the time- and Ca^{2+}-dependent properties of its molecular structure. Accordingly, we focus here on the new elements of a mechanistic understanding of CAM function that emerge from this information and on computational simulation approaches that are well suited for the analysis and interpretation of such data. We review some key aspects of the recent progress made in the elucidation of the structural and dynamic properties of CAM and their putative relations to the functional role of CAM in physiological processes. Special attention is given to the emergence of a structure-based hypothesis for selective binding of CAM to the large variety of proteins it modulates and to the role that Ca^{2+}-binding and the

dynamic properties of the protein have in determining CAM selectivity for protein targets.

Ca^{2+}-BINDING AND THE STRUCTURAL PROPERTIES OF CALMODULIN

Structural Dependence of Ca^{2+} Affinities

Detailed information on the three-dimensional structure of CAM at atomic resolution is relatively recent (5, 15) and reveals an architecture that is similar to that described earlier for troponin C (TNC) (38, 39) in the positioning of two Ca^{2+}-binding globular domains linked by a long, solvent-exposed straight helix (see Figure 1). The two calcium-binding motifs in each globular domain are composed of pairs of helix-loop-helix elements known as EF-hands (80, 109), which define a class of calcium-binding proteins comprising an ever growing number of members being identified in a large variety of species (33, 34). The quest for understanding the relationships between Ca^{2+} binding and the physiological functions of the EF-hand proteins led to explorations of the structural properties of these Ca^{2+}-binding motifs (37) and their sequence similarities in a variety of proteins (e.g. see 89, 127). The properties of EF-hand motifs were compared

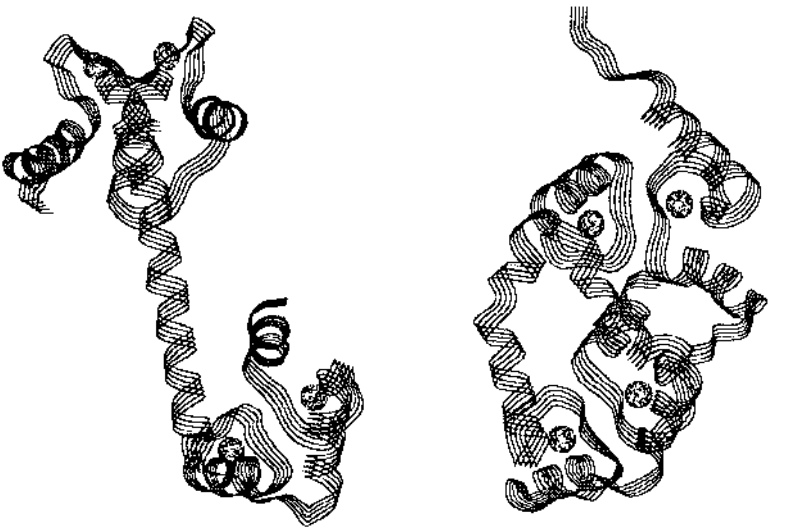

Figure 1 Ribbon tracing of the three-dimensional structure of calmodulin. (*Left: a*) The structure from X-ray crystallography (5). (*Right: b*) The structure computed from molecular dynamics simulation (see CAM2 in Reference 85). To obtain equivalent representations, the Cα carbons of the C-domains (residues 83–148) were superimposed, and the structures were then separated as shown. The Ca^{2+} ions are represented by their van der Waals surfaces.

(80, 109), and the responses of proteins incorporating such specialized motifs to the binding of ions have received special attention (2, 3, 16, 40, 42, 44, 56, 70, 73, 74, 85, 106, 110, 118, 119). Since the activation of CAM is a direct consequence of Ca^{2+}-binding, much attention was also devoted to measuring the kinetics of binding and the affinities of Ca^{2+} for calmodulins from many sources (recent reviews; 16, 22). A number of methods have been used to determine the macroscopic binding constants of CAM (e.g. see 16, 22, 72 and references therein). The results of direct binding studies suggest either four noninteracting sites with identical (or different) Ca^{2+} affinities, or cooperativity between the Ca^{2+} binding sites in at least one of the domains.

Kinetic studies of calcium binding, using $^{43}Ca^{2+}$ NMR and stopped-flow fast kinetics (see 16), led to a model in which Ca^{2+} binds first to the C-terminal domain and subsequently to EF hands I and II in the N-terminal domain when the concentration of Ca^{2+} is increased. Wang et al (131) proposed a model to resolve the discrepancies between the various inferences from the direct binding and the kinetic studies, which assumed two pairs of binding sites with high and low affinity and relatively strong cooperativity in the pair of sites within each domain.

Most of the equilibrium binding studies have suggested varying degrees of positive cooperativity in the binding of Ca^{2+} to the loops of EF-hands III and IV, which have the higher affinity, and some have indicated that cooperativity also is found between the lower affinity sites I and II in the EF-hands of the N-terminal domain (e.g. see 55, 72, 107). The products of the macroscopic binding constants (K_1K_2 of sites III,IV and K_3K_4 of sites I,II in CAM) obtained by Linse et al (72) were considered to be more precisely defined experimentally than the values of the individual binding constants because experimental errors in the latter tended to cancel each other. Comparing the values of these products from various sources (16) does in fact show them to be much closer, at a given ionic strength, than the values of the individual binding constants. The discrepancies in the values of the individual binding constants emphasized in earlier comparisons (e.g. see discussion in 16) could thus be due to greater uncertainties inherent in the experimental procedures, or to the different ways in which binding constants were obtained from the experimental data (16, 72).

To clarify the role of cooperativity between Ca-binding sites in determining the measured affinities, similar studies of Ca^{2+} binding were carried out with tryptic fragments of CAM molecules from various sources (including vertebrate- and yeast-CAM) (58, 72, 106, 113). These fragments (termed TR_1C for residues 1–77, and TR_2C for residues 78–148) are obtained by trypsin digestion that cleaves the central tether helix at Lys77 and separates the pair of EF-hands in the N-terminal domain from those in the C-terminus

(4). A least-squares fitting procedure devised recently to extract the binding constants directly from the experimental data obtained by titration, using ^{1}H-NMR spectroscopy, was applied to CAM and its two tryptic fragments (72). In these studies, the binding constants of Ca^{2+} in each of the fragments were not appreciably different from the values obtained for the corresponding sites in the complete CAM, which indicates no measurable interaction between the N- and C-terminal domains in the Ca-binding process (72). However, some authors have emphasized the experimental difficulties in the interpretation of the measurements yielding the information, e.g. from NMR data (102, 107), of the extent to which the cooperative interaction between the two calcium-binding domains of CAM affects the affinity for Ca^{2+} in the respective binding loops. In yeast-CAM an interaction between the domains seems to affect the Ca^{2+}-binding properties (106), but the amino acid sequence of this CAM form is sufficiently different from vertebrate CAM—especially in the binding loops of the EF-hands—to account for this special behavior. The relation between the Ca^{2+}-binding behavior and the differences observed in the physiological functions of yeast-CAM compared to the vertebrate forms remain unresolved.

Cooperativity and the Time-Dependent Properties of Ca^{2+}-binding Structures

Interest in the determination of the binding constants and the elucidation of inter- and intradomain cooperativity is motivated in part by the expectation that once the binding has been characterized, it may be possible to alter, through selective mutation, both the affinity for Ca^{2+} and the cooperativity, so as to affect the calcium dependence of physiological and pharmacological processes. However, results from the binding studies carried out so far on CAM (see above), as well as on other members of the EF-hand family of Ca-binding proteins (e.g. see 23, 48, 71, 73, 74, 88, 112), have indicated that simply measuring the binding constants is not sufficient for identifying amino acid residues that would be good candidates for effecting a desired change in the calcium-binding properties. Rather, the experimental approaches applied to study the structural consequences of Ca^{2+} binding have disclosed a complex array of structural changes and dynamic responses to the sequential occupation of the calcium-binding sites (e.g. see 3, 11, 24, 25, 27, 41, 65, 74, 84, 104, 105, 125). In some cases, specific mutations in the EF-hands, designed to produce significant effects on Ca^{2+} binding, yielded unexpected results (107, 130). To achieve control of CAM's functions through specifically designed structural modifications will require detailed knowledge of how the binding of Ca^{2+} is controlled by the other parts of the protein's structure that affect the Ca^{2+}-binding elements, and how this structural control is affected by individual amino acid residues.

Recent examples show that such insight at atomic detail can be obtained for the calcium-binding proteins from computational investigations of their structural and dynamic properties (e.g. see 1, 84–86, 92, 111, 118, 137, 138), using molecular simulation techniques that are based on the theoretical methods of classical physics and statistical mechanics. The significant potential of these approaches in the exploration of insights obtained from experimental measurements has been reviewed and evaluated critically (e.g. see 13, 49, 51, 79, 121, 123, 124, 134, 136). To illustrate the nature of the detailed structural and mechanistic information that is attainable from such methods, we briefly review results obtained recently for the small Ca^{2+}-binding protein, calbindin$_{D9k}$, which consists almost entirely of two EF-hand motifs (114).

The effects of Ca^{2+}-binding to calbindin$_{D9k}$ were explored experimentally and computationally to help identify the type of changes in the properties of EF-hand proteins that may determine their function. Calbindin$_{D9k}$ (CAB), the smallest EF-hand protein to be characterized structurally both in the crystal (114) and in solution (2, 105), is a calcium storage protein that binds the two Ca^{2+} ions into EF-hands I and II with a cooperativity of around 1.4 Kcal/mol (70, 73). A recent series of articles (2, 3, 64, 104, 105) report on the structure and internal dynamics of apo-, singly, and doubly occupied CAB, studied using ^{1}H-NMR spectroscopy. A major conclusion from these studies is that the structure of CAB is quite insensitive to the extent of Ca^{2+} occupancy, in contrast to the expectations for Ca-binding regulatory proteins such as CAM. However, these studies found significant effects of Ca^{2+}-binding in the form of a substantially greater degree of flexibility in the apo-form than in either the singly occupied or the holo-form of the protein, and in the modification of the local dynamic properties of the protein (3). The significant reduction in the flexibility of the protein observed with the binding of the first Ca^{2+} led Akke et al (3) to suggest a model in which the main source of cooperativity in the binding of Ca^{2+} to the EF-hands in CAB is the entropic effects arising from changes in the dynamics of the protein with different levels of Ca occupancy.

To explore the detailed effects of Ca^{2+} binding in the EF-hands of CAB on the dynamics of the protein, computational simulations with the methods of molecular dynamics (MD) (12, 13, 51, 124) were carried out (84) on doubly occupied CAB (CAB_2), singly occupied CAB (CAB_1 with Ca^{2+} only in EF-hand II), and apo-CAB (CAB_0). Comparisons of the structures obtained from the MD simulations to the results from NMR and hydrogen exchange measurements of Akke et al (3) showed very good agreement. First, the RMS differences among the three structures obtained from the simulations for the three CAB forms were less than 1.2Å, which indicated the same insensitivity of the structure to changes in Ca^{2+} occupancy as was

observed from the NMR measurements (3). Further agreement between the properties revealed from experimental (3) and computational results (84) was established from comparisons of the observed changes in the local dynamic properties, such as the description of the local unfolding that determines the surface accessibilities of main chain amide groups and is measured by hydrogen exchange rates (see 3 and references therein).

In agreement with Akke et al (3), who concluded that the flexibility of CAB increases in the order $CAB_0 > CAB_1 \geq CAB_2$, the calculated RMS fluctuations of all the protein atoms show the same rank order (84). In addition, both NMR measurements and the simulations indicate that the largest reduction in molecular flexibility takes place with the binding of the first Ca^{2+}, while binding the second Ca^{2+} causes at most a small additional reduction. This agreement between the results from MD simulations and NMR measurements made it attractive to estimate the magnitude of the entropic contribution to the cooperative effect in Ca^{2+}-binding to the EF-hands of CAB. The calculations were based on an approximation of the method proposed by Karplus & Kushick (50), which involved a truncation of the matrix of the covariances of the fluctuations of the atomic coordinates (84). The diagonal elements of the covariance matrix are the mean square fluctuations that increase the configurational entropy, while the off diagonal elements are a measure of the correlations between atomic fluctuations and therefore decrease the entropy. A first approximation of the configurational entropy can be formulated as

$$\Delta S(A \rightarrow B) = R\ln(RMS_B/RMS_A),$$

where the covariance matrix has been condensed to just the average RMS fluctuation of the entire molecule given above. Thus for the binding of the first Ca^{2+}, the entropic contribution becomes (84)

$$\Delta G(CAB_0 \rightarrow CAB_1) = -RT\ln\,[RMS(CAB_1)/RMS(CAB_0)].$$

A similar expression is obtained for binding the second Ca^{2+}, i.e. the process $CAB_1 \rightarrow CAB_2$. However, because the binding of the second Ca^{2+} induces only a small change in flexibility, the latter contribution is negligible. The main entropic component of the free energy of Ca^{2+} binding to CAB obtains from the process $CAB_0 \rightarrow CAB_1$ because the major loss of flexibility is due to binding the first Ca^{2+}. The entropic contribution to the cooperativity is negative because the protein becomes rigid upon Ca^{2+} binding. The calculated values (84) are in reasonably good agreement with the experimental trends, which lends further support to the proposal (3) that cooperativity in CAB is due to the larger change in the dynamic behavior of the

protein that occurs on binding the first calcium, compared to binding the second one.

Such effects of Ca^{2+}-binding on protein dynamics can be expected to occur within the N- and C-terminal domains of CAM, each of which contains a pair of EF-hands. However, the changes induced by Ca^{2+}-binding in the structural properties of CAM that are more directly relevant to its functional properties are also likely to involve the tether helix that determines the mutual orientation and the distance between the two domains (cf the two conformations of CAM in Figure 1). The functional significance of these changes in the mutual orientation of the Ca-binding domains stems from the presence of characteristic hydrophobic regions in these domains. The properties of these regions are modified, as discussed below, in the Ca^{2+}-loaded form of CAM, which prepares the molecule for specific interactions with target proteins.

STRUCTURAL VARIABILITY OF CALMODULIN IN SOLUTION

Comparison of the crystal structure of isolated CAM (5, 15) with the structure obtained from NMR spectroscopy for CAM complexed with M13, a 26-residue peptide representing the CAM-binding region in the enzyme myosin light chain kinase (45, 47), shows two types of structural changes that occur upon complex formation: (*a*) a reorientation of the two globular domains, and (*b*) a compaction of the structure that brings the two domains closer together to envelop and interact with the CAM-binding region of the target protein. Using the four Ca^{2+} ions to define a virtual dihedral angle (as outlined in Reference 92), the reorientation of the domains can be quantified as a change in the angle values from $-134°$ in the crystal structure to 109° in the complex. The compaction is quantifiable through the radius of gyration (e.g. see 31, 85), which decreases from 22 to 17Å.

Experimental approaches have been used to characterize the flexibility of the tether (e.g. see 7, 90) and the departure of the solution structure of uncomplexed CAM from the extended form observed in the crystal (e.g. see 31, 128). The results from small angle X-ray scattering (SAXS) experiments, which suggest some compaction of CAM in solution relative to the crystal structure, were somewhat inconclusive since different authors did not agree in their interpretation of the SAXS results (31, 101). We showed, however, that the observed solution pair distribution function of CAM obtained from SAXS experiments (e.g. see 31, 77) could be rationalized by assuming an equilibrium between structures in various states of reorientation and compaction (85) (the compacted structure shown in Figure 1 *right* illustrates one of the conformations visited by CAM). This obser-

vation agrees with results from NMR spectroscopy (7) and with inferences from energy transfer studies on CAM and troponin-C, which indicate that the two lobes move closer together when the pH is raised from 5.5 to 7.4 (e.g. see 128,129).

The agreement between observations from experiment and from computational simulation, which suggests that the structure of CAM in solution can access various configurations and the potential importance of this dynamic variability in structure for the function of CAM, made it worthwhile to inquire how this flexibility is controlled. The exploration of the mechanism by which the structural elements of CAM and their interactions determine the time-dependent behavior of the molecule was carried out by analyzing the dynamic structural details provided by the MD simulations (92).

A Mechanism of Compaction

Careful analysis of the time evolution of interactions between individual amino acid residues comprising the peptide chain from several MD trajectories (92) revealed a pattern of H-bonds that form and are severed during the simulations. A structural analysis of these time-dependent H-bonding patterns was carried out (92) to determine whether any could be directly involved in facilitating the compaction process. The formation of H-bonds, which connected groups in different elements of secondary structure and persisted for a long simulation period, were deemed the most likely candidates for key interactions in the compaction mechanism because these would be the most likely to stabilize structural changes.

The analysis identified three arginine residues (Arg74, Arg 86, and Arg90), which appeared to be involved in H-bonding patterns that met the criteria defined above. Typical in this context was the behavior of Arg74, which was found to form a new H-bond to the carbonyl group of Val55 (see hydrogen-bonding patterns in Figure 2) after only 18.5 psec of simulation and to maintain other interactions, all in a manner suggestive of a reversible compaction trigger (see below). The bond to Val55 forms at a time when the orientation of the globular domains begins to change from the *trans*-like orientation observed in the X-ray structure to one that is more *cis*-like. Figure 2 shows that the H-bond to Glu67 persists throughout the early part of the trajectory, but breaks sometime between 29 and 85 psec into the trajectory. Also in that time period, an additional H-bond forms with Glu54. The H-bonding pattern of Arg74 shares a characteristic of all three arginines, namely, an H-bond anchoring the residue to a nearby residue (Thr70 for Arg74). The pattern of first latching onto Glu67, then Val55, with the bond to Glu67 subsequently being broken and replaced by an attachment to Glu54, is suggestive of a ratcheting process where one end of the chain remains firmly anchored (to Thr70) and the other end of the

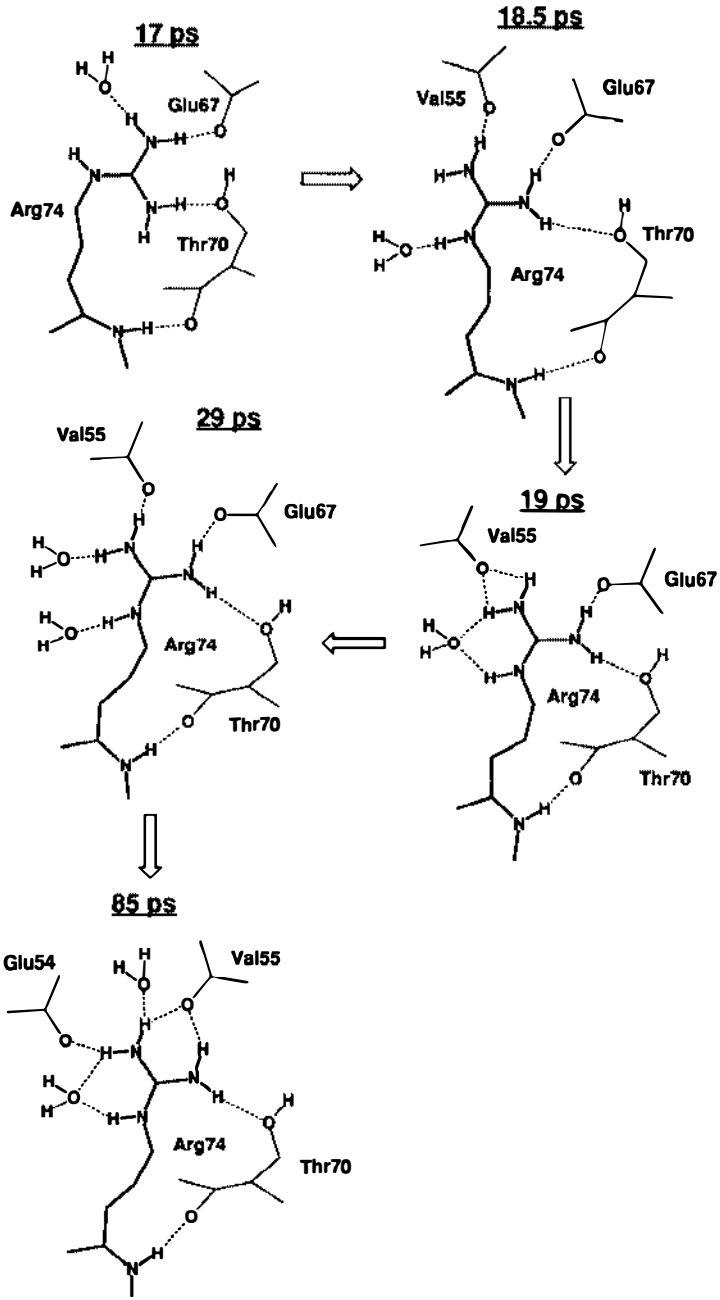

Figure 2 Schematic representation of the time-dependent evolution of the hydrogen bonding pattern involving Arg74 in molecular dynamics simulations of calmodulin. The two-dimensional structural representation is derived from snapshots of the structure taken at successive stages of the simulation. (*Top left*) at 17 psec; (*top right*) at 18.5 psec; (*middle right*) at 19 psec; (*middle left*) at 29 psec; (*lower left*) at 85 psec.

residue draws in successive attachment sites from more distant parts of the structure.

Several additional noteworthy aspects of the involvement of Arg74 in the compaction process may be seen from Figure 2. At all times there are at least two residues attached to the guanidinium moiety of Arg74, and from 19 psec onward all the guanidinium protons are involved in H-bonding. Perhaps in this way the potential for this group to stabilize intermediate structures is optimally exploited. Also of interest is the involvement of waters in the dynamics of the H-bonding patterns. Figure 2 shows that waters were involved in the H-bonding process and, in fact, continuously surrounded Arg74 (see 92).

A similar H-bonding pattern was also observed for Arg90, which was anchored to Glu87, with the residues involved in the ratcheting process including Asn97 and Gly96. At one point in the trajectory the carbonyl oxygen of Arg86 was linked to Arg90, thus forming a common H-bonding network, perhaps coordinating the movement of both. In these two latter cases, water again participated intimately in the continuously altering H-bonding networks. Finally, it is noteworthy that for both Arg74 and Arg90, residues from the Ca^{2+}-binding loops were involved in the H-bonding patterns, and that the time evolution of the interaction energies of Arg74 and Arg90 with the rest of the protein structure (see 92) also supported their involvement in the compaction process. The function of Arg74 and Arg90 in facilitating the reversible compaction appeared the clearest, but the role of Arg86 was not clear, i.e. whether it was driving or responding to structural change.

To test how essential these residues are for compaction, the simulation was repeated, but in each run, one of these residues was mutated to alanine. Thus three additional simulations were carried out (K Haydock et al, unpublished) for the three mutated forms of CAM: Arg 74 to Ala74 (R74A), Arg86 to Ala86 (R86A), and Arg90 to Ala90 (R90A), using identical simulation conditions as one of the simulations on wild-type CAM, which yielded a compacted structure (i.e. CAM10 in Reference 92). In all three mutations, the two lobes of CAM reoriented: for the wild-type CAM, the virtual dihedral angle between the four Ca^{2+} (see above) was $-72°$, and for the three mutants, the values were -77, 18, and $-43°$ for R74A, R86A, and R90A, respectively). The R74A mutant assumed nearly the same orientation as the wild-type CAM. The domains of the R86A mutant assumed quite a different disposition, but one that is close to the orientation from another simulation on the wild-type protein in which the conditions were altered (see Table 1 in Reference 85). The R90A mutant achieved an interdomain orientation intermediate between R74A and R86A. However, only R86A compacted, whereas both R74A and R90A became somewhat more extended than the starting (X-ray) structure. The simulations therefore

indicate that Arg74 and Arg90 (perhaps in concert with Arg86), but not Arg86 alone, are essential for compaction. The H-bonding patterns around the residues that were not mutated still underwent the characteristic changes described above for the simulation on the wild type, but when one of the two essential residues (Arg74 or Arg90) was absent, compaction did not occur.

It is also noteworthy that both Arg74 and Arg90 seemed to contribute in important ways to the stability of the structure. Thus the CAM mutants R74A and R90A exhibited large and persistent fluctuations in their radii of gyration and in their interdomain orientations over relatively long periods of time. In contrast, the structural changes in the simulations of the wild-type CAM and the R86A mutant always took place in the first part of the run (although these changes took longer in some cases than in others), and subsequently the overall structures remained quite stable in the compacted form. These observations help support the main conclusion of these computer mutation experiments, namely that Arg74 and Arg90 play crucial roles in controlling the molecular flexibility that CAM requires for its functional viability.

THE TIME-DEPENDENT STRUCTURE OF HYDROPHOBIC PATCHES IN CALMODULIN

An early observation from experimental studies of structure-function relationships in CAM was the exposure to the solvent environment of clusters of hydrophobic residues following the binding of Ca^{2+} (e.g. see 67, 115). The steric adjacency of these hydrophobic residues caused these regions to be viewed as hydrophobic patches. Biochemical experiments, as well as structure determinations, have implicated these hydrophobic patches in the mode of action of CAM in the cell (90, 91, 115, 116). The recent structure of CAM complexed to a peptide (M13) representing the binding domain of skeletal muscle myosin light chain kinase (MLCK), obtained from NMR spectroscopy (45) and from X-ray crystallography (81), confirms the importance of interactions between specific hydrophobic residues in CAM and its target protein. As it becomes clear that degrees of Ca^{2+} occupancy determine both structural and dynamic properties of EF-hand proteins (see section above), the nature of the relationship between Ca-binding and the induced, specific structural changes in the hydrophobic patches becomes a tantalizing question. Significant insight into this question can be gained by examining the structural details of these patches, which are so intimately related to CAM/target binding, and by comparing their disposition in the CAM structures from X-ray crystallography, from NMR spectroscopy, and from computational simulations. An important consideration here is that

both X-ray crystallography and NMR spectroscopy provide a time-averaged picture of the disposition of the hydrophobic patches, whereas the simulations provide the additional insight of the time evolution of the structural changes. As discussed below, it is the availability of this information on structural dynamics that allows the formulation of a mechanism for target selectivity in the actions of CAM.

Selectivity in CAM Binding to Target Proteins

Figure 3a-d displays space-filling CPK representations of the molecular structure of CAM for a comparison of the hydrophobic patches in the molecular structures obtained from crystallography (5), NMR spectroscopy (45), and computational simulations (85, 92), respectively. Only the N-ter-

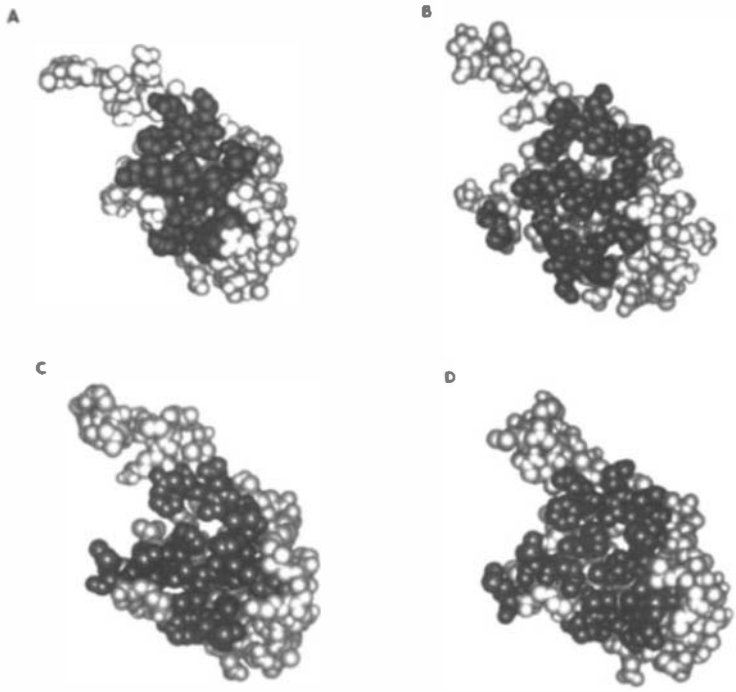

Figure 3 Space filling representations of the target-binding face of the N-terminal domain in various conformations of calmodulin. (*a*) The crystallographic structure (as in Figure 1 left). (*b*) The structure from NMR spectroscopy (45). (*c*) The structure from molecular dynamics simulation (as in Figure 1 right). (*d*) The structure obtained from an alternative molecular dynamics simulation (92). Atoms involved in interactions with the M13 peptide from the CAM-binding domain of skeletal muscle myosin light chain kinase (residues 577–602) are darkly shaded; the other atoms are lightly shaded. Residues 12–76 in all the CAM structures shown were superimposed on the N-terminal segment of the structure from NMR spectroscopy to obtain the equivalent views shown.

minal segment (residues 1–76) is shown, in a perspective that is "looking into" the domain head-on (the tether, residues 77–83, is included in the Kendrew representation). To secure the same orientation in the display of each structure, residues 12–76 of the structures from the crystal and from the computational simulations were superimposed on the corresponding segment of the N-terminal domain of the NMR structure. Charged and polar residues, as well as hydrophobic residues (dark area in Figure 3) have been identified from the NMR studies (45) as being involved in binding to M13. The exposed surfaces of these polar and hydrophobic residues provide regions of interaction with the target peptide and constitute a surface area relevant to binding (SARB). The SARB is defined quantitatively for the interaction of CAM with M13 by taking the difference in solvent accessible surface area between the CAM/M13 holo- and apo- structures (i.e. the NMR structure with and without the M13 peptide).

The overall configuration of the residues in the SARB, with the hydrophilic residues framing several hydrophobic regions on the outside, is similar in all the cases shown. Nevertheless, there are several key differences: comparison of the structures from X-ray crystallography and NMR spectroscopy reveals that in the latter structure the entire domain appears to span a larger space, albeit with several holes; importantly, the disposition of the hydrophobic patches differs in the crystal and in solution. In the NMR structure in solution, the patches have spread out and form several distinct islands. The conformations of the hydrophilic residues have also changed, and in the particular view shown, the Ca^{2+} ion is accessible to the solvent in the NMR structure, but not in the crystal structure.

The SARB construct defined for the particular M13 target makes it possible to track the time-dependent developments in the target-binding potential of CAM by following its behavior in a computational simulation of CAM dynamics. The working hypothesis is that the accessibility of this surface area, which is relevant to the binding of a particular target, will change with time, as it changes with the binding of Ca^{2+} and of various peptides (e.g. see 46, 52-54, 67, 115, 119). The mechanistic implication is that the dynamic changes in the SARB will determine the time-dependence of the binding probability for certain targets. As different targets are likely to require different SARB, these changes are likely to constitute a time-dependent (and Ca^{2+} occupancy-dependent) scheme for achieving selectivity in the physiological actions of CAM.

It is clear from Figure 3 that the three-dimensional configuration of the SARB for M13 defined from the NMR structure is different from the surface outlined by the same residues in the crystal structure of CAM. Examination of the same area in the results from the MD simulations performed on isolated CAM (with various solvent models, but no binding

peptides or inhibitors) provides SARB shapes that are time-dependent. An average structure (obtained from the last part of the simulation trajectory) could mimic the properties of a relevant SARB conformation. However, in the absence of a target protein, the hydrophobic patches would evolve further to what could become a nonbinding configuration. The results of the computational simulation can be explored for the time-dependent appearance of the appropriate SARB configuration. For example, such a search for potentially significant structures was performed on the trajectory of the computational simulations by comparing the developments in the SARB, starting from the crystal structure (5) (which is the starting point for the dynamics simulations) (85, 92) and going towards the structure of CAM in the complex with M13 from the NMR measurement (45). To quantify the changes, a numerical value was calculated for the solvent-accessible-surface area (SASA) using the GEPOL algorithm (93, 103). The SASA of the 39 interacting residues in the SARB was calculated for the NMR and crystal structures of CAM, and it was found that the SASAs of 28 residues were larger in the NMR than in the crystal structure, while in the remaining 11 residues the SASAs of the NMR structure were smaller. The SASAs for a series of snapshots from several dynamics trajectories were calculated for each of the 39 interacting residues, and the value was compared to the SASAs obtained for these residues in the X-ray structure and checked for qualitative agreement with the trend found for the change in SASAs between the NMR and crystal structures. The agreement in the preparation of the SARB for binding (i.e. the transition from the crystal structure to the NMR structure) tended to improve early in the trajectory, persisted briefly, and then became less good. For example, for CAM10 (defined in Reference 92), the change in SASA was correctly predicted for 20 residues from the snapshot at 20 psec, 27 residues were correctly predicted at 40 psec, but for the average structure obtained from the last part of the simulation (286–326 psec), the agreement was reduced to 24 residues. This trend was observed for all the trajectories examined, independently of how well the changes in accessible surface area agreed with the observed changes between the NMR and crystal structures. However, it is important to emphasize that even the final average structures resulting from the computational simulations maintain a SARB that is closer to that defined by the NMR structure than the crystal structure. Thus in both CAM2 and CAM10 structures (see 85, 92, respectively), the patches have spread out relative to the X-ray structure, with the tendency to form islands similar to those seen in the NMR structure. This further illustrates the agreement between the computed and observed structures and lends support to the analysis of the time-dependent features in the SARB defined for CAM from computational studies.

The Role of the Central Tether Helix in the Interactions of CAM with Its Targets

Residues 73–82 constitute the tether connecting the two Ca^{2+}-binding domains on which the SARB for a specific target can be identified. This tether region is helical in the crystal structure of CAM, but dissolves into a flexible loop in the complex with M13 (45, 47, 81). In both the CAM2 and CAM10 structures obtained from the computational simulations (85, 92), this is also an important region of flexible structural rearrangement that contributes to the reorientation of the domains and to subsequent compaction (e.g. see Figure 1 *right*). The special dynamic properties of this region were also identified in the NMR structure of the uncomplexed CAM (7). It is of interest that between residues 73 to 82, only Met76 and Ser81 interact with M13 and, in fact, their interaction is marginal because binding of M13 decreases the SASA of these two residues by less than 4% even though about 80% of the maximum SASA is exposed in the apo-NMR structure. This lack of interaction between M13 and the tether suggests that the structural change observed between the crystal and NMR structures of the CAM/M13 complex is not the result of interactions of M13 with the tether. This conclusion is supported by two further observations: first, structures obtained from various trajectories suggest that CAM's flexibility may result from distortions in different parts of the linker (92). Moreover, as mentioned above, the pair distribution functions observed from SAXS experiments in solution (31, 77) can be rationalized as we described (85) by assuming an equilibrium between structures in various states of compaction and reorientation. Second, the Ca-binding studies by Forsen et al (e.g. see 72, 73) discussed above failed to detect interdomain cooperativity in the binding. Certainly, a very flexible tether, which assumes a continuously variable range of conformations in solution (7), is unlikely to be involved in transmitting information between the two lobes. Rather, the early observations of the importance of such flexibility (e.g. see 90, 91, 94, 95) are likely to reflect the role of the flexible tether in placing the SARBs (evolving in the two separate domains) into positions appropriate for interaction with the target (for some recent discussions, see 30, 87, 99). Early mutation studies designed to determine the functional significance of the central helix of CAM (96) reached similar conclusions with regard to the role of this structure in the appropriate positioning of the sites required for specific interaction with the target protein.

Since the exposure of hydrophobic residues in the crystal and NMR structures was similar, the prediction from model building of the residues that interact with such peptides as M13 (e.g. see 91, 94) or with CAM inhibitors (108) was quite successful. In the specific case of M13, it was

necessary to assume some deformation of CAM in order to bring the domains closer together, and here the modeling was less successful (assuming a single kink in Ser81), since both the NMR and the crystal data for the complex (45, 81) ultimately showed that the domains came closer together because the tether was deformed into an extended loop with complete loss of helicity. The structures generated by the dynamics calculations predicted (85, 92) that compaction resulted from tether distortion over its entire length (residues 73–84), a development that is much closer to the dissolution exhibited by the NMR structures (7, 45) than the models that assumed a localized kink resulting from an alteration in the ϕ and ψ angles of a single residue. This difference in results obtained from model building compared to computational simulation clearly illustrates the advantage of the latter (see also 137), in which the time evolution of the structure is obtained through a straightforward application of Newton's laws of motion, and the inherent approximations and errors are, in principle, correctable (e.g. see 13, 51, 68, 78, 79, 121–124, 132–134).

CONCLUDING REMARKS

The mechanistic insight provided by the analysis of structure and dynamics of the CAM molecule outlined in this review suggests several novel possibilities for modulating the physiological functions of CAM. First, of course, is alteration of Ca^{2+} binding. An obvious approach is to alter one or more residues in the Ca-binding regions but, as discussed here, attempted changes through mutations suggested by the average structure of the molecule have not always led to the expected results. An alternative, more subtle type of structural manipulation, suggested from the results of the computational simulations would be to change the dynamic behavior of the apo-structure relative to the fully Ca^{2+}-loaded CAM. The specific modifications can be probed with computational simulations, and the results can be directly tested experimentally. However, the mechanisms of the measured effects on activity may still be difficult to interpret because at present it is not clear which of the two components of the structural dynamics, i.e. compaction in solution, or flexibility (or both), is the controlling factor in CAM's activity. The most complex, but perhaps the most effective, mutations would be aimed at altering the structures of the hydrophobic patches. Here, the simulation techniques might be an extremely powerful tool in searching for effective mutations, since the experimental or modeling approaches would essentially have to proceed by trial and error.

From this review it should be clear that the study of the structural and dynamic properties of calmodulin and related Ca-binding proteins provides a potentially rich source for gaining the type of mechanistic insights that

will be required to implement structurally defined design strategies (138) in developing engineered proteins with desirable properties. At the same time, it is evident that the application of computer simulation techniques to this class of proteins has only just begun and that considerable work will be required to provide a generally useful body of mechanistic information. The main motivation for continuing this effort is that these techniques reveal time-dependent structural properties that appear to be crucial to the behavior of the system and are more difficult to evaluate with other methods.

ACKNOWLEDGMENTS

Critical reading of the manuscript by Dr. JN Kushick is gratefully acknowledged. The authors' work was supported in part by National Institutes of Health grants GM-41373, and DA-00060. Computations were performed on the supercomputer systems at the Pittsburgh Supercomputer Center (sponsored by the National Science Foundation), the Cornell National Supercomputer Facility (sponsored by the National Science Foundation and IBM), the Advanced Scientific Computing Laboratory at the Frederick Cancer Research Facility of the National Cancer Institute (Laboratory for Mathematical Biology), and the University Computer Center of the City University of New York.

Literature Cited

1. Ahlstrom P, Teleman O, Kordell J, Forsen S, Jonsson B. 1989. A molecular dynamics simulation of bovine calbindin$_{D9k}$. Molecular structure and dynamics. *Biochemistry* 28:3205–11
2. Akke M, Drakenberg T, Chazin WJ. 1992. Three-dimensional solution structure of Ca^{2+}-loaded porcine calbindin$_{D9k}$ determined by NMR spectroscopy. *Biochemistry* 31:1011–20
3. Akke M, Forsen S, Chazin WJ. 1991. Molecular basis for co-operativity in Ca^{2+} binding to calbindinD9k. *J. Mol. Biol.* 229:173–89
4. Andersson A, Forsen S, Thulin E, Vogel HJ. 1983. Cadmium-113 nuclear magnetic resonance studies of proteolytic fragments of calmodulin: Assignment of strong and weak binding sites. *Biochemistry* 22:2309–13
5. Babu YS, Bugg CE, Cook WJ. 1988. Structure of calmodulin refined at 2.2 Å resolution. *J. Mol. Biol.* 204:191–204
6. Bading H, Ginty DD, Greenberg ME. 1993. Regulation of gene expression in hippocampal neurons by distinct calcium signalling pathways. *Science* 260:181–86
7. Barbato G, Ikura M, Kay LE, Pastor RW, Bax A. 1992. Backbone dynamics of calmodulin studied by ^{15}N relaxation using inverse detected two-dimensional NMR spectroscopy: The central helix is flexible. *Biochemistry* 31:5269–78
8. Bartelt DC, Fidel S, Farber LH, Wolff DJ, Hammell RL. 1988. Calmodulin-dependent protein kinase in *Aspergillus nidulans*. *Proc. Natl. Acad. Sci. USA* 85:3279–83
9. Beckingham K. 1991. Use of site-directed mutations in the individual Ca^{2+}-binding sites of calmodulin to examine Ca^{2+}-induced conformational changes. *J. Biol. Chem.* 266:6027–30
10. Bowman BR, Peterson JA, Stull JT. 1992. Pre-steady-state kinetics of the activation of rabbit skeletal muscle myosin light chain kinase by Ca^{2+}/calmodulin. *J. Biol. Chem.* 267: 5346–54
11. Brito RMM, Putkey JA, Strynadka

NCJ, James MNG, Rosevear PR. 1991. Comparative NMR studies on cardiac troponin C and a mutant incapable of binding calcium at site II. *Biochemistry* 30:10236–45

12. Brooks BR, Bruccoleri RE, Olafson BD, States DJ, Swaminathan S, et al. 1983. CHARMM: A program for macromolecular energy, minimization and dynamics calculations. *J. Comput. Chem.* 4:187–217
13. Brooks CL, Karplus M, Pettitt BM. 1988. *Proteins: A Theoretical Perspective of Dynamics, Structure, and their Thermodynamics,* New York: Wiley & Sons. 259 pp.
14. Chapman ER, Alexander K, Vorherr T, Carafoli E, Storm DR. 1992. Fluorescence energy transfer analysis of calmodulin-peptide complexes. *Biochemistry* 31:12819–25
15. Chattopadhyaya R, Meador WE, Means AR, Quiocho FA. 1992. Calmodulin structure refined at 1.7A resolution. *J. Mol. Biol.* 228:1177–92
16. Cox JA, Comte M, Mamar-Bachi A, Milos M, Schaer J-J. 1988. Cation binding to calmodulin and relation to function. In *Calcium and Calcium Binding Proteins,* ed. C Gerday, L Bolis, R Gilles, pp. 141–62. New York: Springer Verlag
17. Craig TA, Watterson DM, Prendergast FG, Haiech J, Roberts DM. 1987. Site-specific mutagenesis of the alpha-helices of calmodulin. *J. Biol. Chem.* 262:3278–84
18. Davis JRE, Hoggard N, Wilson EM, Vidal ME, Sheppard MC. 1991. Calcium/calmodulin regulation of the rat prolactin gene is conferred by the proximal enhancer region. *Mol. Endocrinol.* 5:8–12
19. Davis TN. 1992. What's new with calcium? *Cell* 71:557–64
20. Evered D, Whelan J, eds. 1986. *Calcium and the Cell.* New York: Wiley & Sons
21. Fitzsimons DP, Herring BP, Stull T, Gallagher PJ. 1992. Identification of basic residues involved in activation and calmodulin binding of rabbit smooth myosin light chain kinase. *J. Biol. Chem.* 267:23903–9
22. Forsen S, Linse S, Drakenberg T, Kordel J, Akke M, et al. 1991. Ca^{2+} binding in proteins of the calmodulin superfamily: cooperativity, electrostatic contributions and molecular mechanisms. In *Protein Conformation,* ed. DJ Chadwick, K Widdows, pp. 222–36. Chichester: Wiley & Sons
23. Forsen S, Linse S, Thulin E, Lindegard B, Martin SR, et al. 1988. Kinetics of calcium binding to calbindin mutants. *Eur. J. Biochem.* 177:47–52
24. Fujimori K, Sorenson M, Herzberg O, Moult J, Reinach FC. 1990. Probing the calcium-induced conformational transition of troponin C with site-directed mutants. *Nature* 345:182–84
25. Geiser JR, van Tuinen D, Brockerhoff SE, Neff MM, Davis TN. 1991. Can calmodulin function without binding calcium? *Cell* 65:949–59
26. Gerday C, Bolis L, Gilles R, eds. 1988. *Calcium and Calcium Binding Proteins.* Berlin: Springer
27. Grabarek Z, Leavis PC, Gergely J. 1986. Calcium binding to the low affinity sites in troponin C induces conformational changes in the high affinity domain. A possible route of information transfer in activation of muscle contraction. *J. Biol. Chem.* 261:608–13
28. Hahn K, DeBiasio R, Taylor DL. 1992. Patterns of elevated free calcium and calmodulin activation in living cells. *Nature* 359:736–38
29. Hanson PI, Schulman H. 1992. Neuronal Ca^{2+}/calmodulin-dependent protein kinases. *Annu. Rev. Biochem.* 61:559–601
30. Head JF. 1992. A better grip on calmodulin: Two atomic resolution structures show just how calmodulin binds to a peptide that represents the natural binding of a calmodulin-activated enzyme. *Curr. Biol.* 2:609–11
31. Heidorn DB, Trewhella J. 1988. Comparison of the crystal and solution structures of calmodulin and troponin C. *Biochemistry* 27:909–15
32. Heidorn DB, Seeger PA, Rokop SE, Blumenthal DK, Means, AR, et al. 1989. Changes in the structure of calmodulin induced by a peptide based on the calmodulin-binding domain of myosin light chain kinase. *Biochemistry* 28:6757–64
33. Heizmann CW, ed. 1991. *Novel Calcium-Binding Proteins.* New York: Springer-Verlag. 624 pp.
34. Heizmann CW, Hunziker W. 1991. Intracellular calcium-binding proteins: more sites than insights. *Trends Biochem. Sci.* 16:98–103
35. Hennessey JP, Manavalan P, Johnson WC, Malencik DA, Anderson SR, et al. 1987. Conformational transitions of calmodulin as studied by vacuum-UV CD. *Biopolymers* 26:561–71
36. Herring BP, Gallagher PJ, Stull JT. 1992. Substrate specificity of myosin

light chain kinases. *J. Biol. Chem.* 267:25945–50
37. Herzberg O, Jamcs MNG. 1985. Common structural framework of the two Ca^{2+}/Mg^{2+} binding loops of troponin C and other Ca^{2+} binding proteins. *Biochemistry* 24:5298–302
38. Herzberg O, James MNG. 1985. Structure of the calcium regulatory muscle protein troponin C at 2.8A resolution. *Nature* 313:653–59
39. Herzberg O, James MNG. 1988. Refined crystal structure of troponin C from turkey skeletal muscle at 2.0A resolution. *J. Mol. Biol.* 203:761–79
40. Herzberg O, Moult J, James MNG. 1986. A model for the Ca^{2+}-induced conformational transition of troponin C. A trigger for muscle contraction. *J. Biol. Chem.* 261:2638–44
41. Hinrichsen R, Wilson E, Lukas T, Craig T, Schultz J, et al. 1990. Analysis of the molecular basis of calmodulin defects that affect channel-mediated cellular responses: site-specific mutagenesis and microinjection. *J. Cell Biol.* 111:2537–42
42. Hori K, Kushick JN, Weinstein H. 1988. Structural and energetic parameters of Ca^{2+} binding to peptides and proteins. *Biopolymers* 27:1865–86
43. Hsu Y-T, Molday RS. 1993. Modulation of the cGMP-gated channel of rod photoreceptor cells by calmodulin. *Nature* 361:76–79
44. Iida S, Potter JD. 1986. Calcium binding to calmodulin. Cooperativity of the calcium-binding sites. *J. Biochem. (Tokyo)* 99:1765–72
45. Ikura M, Clore GM, Gronenborn AM, Zhu G, Klee CB, Bax A. 1992. Solution structure of a calmodulin-target peptide complex by multidimensional NMR. *Science* 256:632–38
46. Ikura M, Hiraoki T, Hikichi K, Mikuni T, Yazawa M, et al. 1983. Nuclear magnetic resonance studies on calmodulin: Calcium-induced conformational change. *Biochemistry* 22: 2573–79
47. Ikura M, Kay LE, Krinks M, Bax A. 1991. Triple-resonance multidimensional NMR study of calmodulin complexed with the binding domain of skeletal muscle myosin light-chain kinase: Indication of a conformational change in the central helix. *Biochemistry* 30:5498–504
48. Imaizumi M, Tanokura M, Yamada K. 1987. A calorimetric study on calcium binding by troponin C from bullfrog skeletal muscle. *J. Biol. Chem.* 262:7963–66
49. Jonsson B, ed. 1989. *Structure and Dynamics in Biological Systems*. Cambridge/New York: Cambridge Univ. Press
50. Karplus M, Kushick JN. 1981. Methods for estimating the configurational entropy of macromolecules. *Macromolecules* 14:325–32
51. Karplus M, Petsko GA. 1990. Molecular dynamics simulations in biology. *Nature* 347:631–39
52. Kataoka M, Head JF, Seaton BA, Engelman DM. 1989. Melittin binding causes a large calcium-dependent conformational change in calmodulin. *Proc. Natl. Acad. Sci. USA* 86:6944–48
53. Kataoka M, Head JF, Vorherr T, Krebs J, Carafoli E. 1991. Small-angle X-ray scattering study of calmodulin bound to two peptides corresponding to parts of the calmodulin-binding domain of the plasma membrane Ca^{2+} pump. *Biochemistry* 30:6247–51
54. Kawasaki Y, Van Eerd JP. 1972. The effect of Mg^{2+} on the conformation of the Ca^{2+}-binding component of troponin. *Biochem. Biophys. Res. Commun.* 49:898–905
55. Kilhoffer M-C, Kubina M, Travers F, Haiech J. 1992. Use of engineered proteins with internal tryptophan reporter groups and perturbation techniques to probe the mechanism of ligand-protein interactions: Investigation of the mechanism of calcium binding to calmodulin. *Biochemistry* 31:8098–106
56. Klee CB. 1988. Interaction of calmodulin with Ca^{2+} and target proteins. In *Calmodulin*, ed. P Cohen, CB Klee, pp. 35–56. Amsterdam: Elsevier
57. Klee CB, Crouch TH, Richman PG. 1980. Calmodulin. *Annu. Rev. Biochem.* 49:489–515
58. Klee CB, Newton DL, Ni W-C, Haiech J. 1986. Regulation of the calcium signal by calmodulin. See Ref. 20, pp. 162–82
59. Klee CB, Vanaman TC. 1982. Calmodulin. *Adv. Protein Chem.* 35:213–303
60. Klevit RE. 1981. *A study of calmodulin in solution using high resolution* ^{1}H NMR. PhD thesis. Oxford Univ., Oxford. 173 pp.
61. Klevit RE. 1987. Study of calmodulin—peptide interactions by NMR spectroscopy. *Methods Enzymol.* 139: 197–206
62. Klevit RE, Blumenthal DK, Wemmer DE, Krebs EG. 1985. Interaction of calmodulin and a calmodulin-binding peptide from myosin light chain kinase:

Major spectral changes in both occur as the result of complex formation. *Biochemistry* 24:8152–57

63. Klevit RE, Dalgarno DC, Levine BA, Williams RJP. 1984. H-NMR studies of calmodulin—the nature of the Ca^{2+}-dependent conformational change. *Eur. J. Biochem.* 139:109–14
64. Kordel J, Forsen S, Drakenberg T, Chazin WJ. 1990. The rate and structural consequences of proline cis-trans isomerization in calbindin$_{D9k}$: NMR studies of the minor (cis-Pro43) isoform and the Pro43Gly mutant. *Biochemistry* 29:4400–409
65. Krudy GA, Brito RMM, Putkey JA, Rosevear PR. 1992. Conformational changes in the metal-binding sites of cardiac troponin C induced by calcium binding. *Biochemistry* 31:1595–602
66. Kung C, Preston RR, Maley ME, Ling K-Y, Kanabrocki JA, et al. 1992. In vivo *Paramecium* mutants show that calmodulin orchestrates membrane responses to stimuli. *Cell Calcium* 13: 413–25
67. LaPorte DC, Wierman BM, Storm DR. 1980. Calcium-induced exposure of a hydrophobic surface on calmodulin. *Biochemistry* 19:3814–19
68. Levitt M, Sharon R. 1988. Accurate simulation of protein dynamics in solution. *Proc. Natl. Acad. Sci. USA* 85:7557–61
69. Ling K-Y, Preston RR, Burns R, Kink JA, Saimi Y, et al. 1992. Primary mutations in calmodulin prevent activation of the Ca^{2+}-dependent Na^{+} channel in *Paramecium*. *Proteins: Struct. Funct. Gen.* 12:365–71
70. Linse S, Brodin P, Drakenberg T, Thulin E, Sellers P, et al. 1987. Structure-function relationships in EF-hand Ca^{2+}-binding proteins. Protein engineering and biophysical studies of calbindin$_{D9k}$. *Biochemistry* 26: 6723–35
71. Linse S, Brodin P, Johansson C, Thulin E, Grundstrom T, et al. 1988. The role of protein surface charges in ion binding. *Nature* 335:651–52
72. Linse S, Helmersson A, Forsen S. 1991. Calcium binding to calmodulin and its globular domains. *J. Biol. Chem.* 266:8050–54
73. Linse S, Johansson C, Brodin P, Grundstrom T, Drakenberg, T, et al. 1991. Electrostatic contributions to the binding of Ca^{2+} in calbindin$_{D9k}$. *Biochemistry* 30:154–62
74. Linse S, Teleman O, Drakenberg T. 1990. Ca^{2+} binding to calbindin D9k strongly affects backbone dynamics: Measurements of exchange rates of individual amide protons using ^{1}H NMR. *Biochemistry* 29:5925–34
75. Lu KP, Rasmussen CD, May GS, Means AR. 1992. Cooperative regulation of cell proliferation by calcium and calmodulin in *Aspergillus nidulans*. *Mol. Endocrinol.* 6:365–74
76. Lukas TJ, Wallen-Friedman M, Kung C, Watterson DM. 1989. In vivo mutations of calmodulin: A mutant *Paramecium* with altered ion current regulation has an isoleucine-to-threonine change at residue 136 and an altered methylation state at lysine residue 115. *Proc. Natl. Acad. Sci. USA* 86:7331–35
77. Matsushima N, Izumi Y, Matsuo T, Yoshino H, Ueki, T, et al. 1989. Binding of both Ca^{2+} and mastoparan to calmodulin induces a large change in tertiary structure. *J. Biochem.* 105: 883–87
78. McCammon JA. 1987. Computer-aided molecular design. *Science* 238:486–91
79. McCammon JA, Harvey SC. 1987. *Dynamics of Proteins and Nucleic Acids*, New York: Cambridge Univ. Press. 234 pp.
80. McPhalen CA, Strynadka NCJ, James MNG. 1991. Calcium binding sites in proteins: A structural perspective. *Adv. Protein Chem.* 42:77–144
81. Meador WE, Means AR, Quiocho FA. 1992. Target enzyme recognition by calmodulin: 2.4Å structure of a calmodulin-peptide complex. *Science* 257: 1251–55
82. Means AR, Conn PM, eds. 1987. *Cellular Regulators. Part A. Calcium- and Calmodulin-Binding Proteins.* New York: Academic. 917 pp.
83. Means AR, VanBerkum MFA, Bagchi IC, Lu KP, Rasmussen, CD. 1991. Regulatory functions of calmodulin. *Pharmacol. Ther.* 50:255–70
84. Mehler EL, Kushick JN, Weinstein H. 1993. Consequences of sequential Ca^{2+} occupancy for the structure and dynamics of calbindinD9k: Computational simulations and comparison to experimental determinations in solution. *Mol. Simulation.* 10:309–34
85. Mehler EL, Pascual-Ahuir JL, Weinstein H. 1991. Structural dynamics of calmodulin and troponin C. *Protein Eng.* 4:625–37
86. Mehler EL, Solmajer T. 1991. Electrostatic effects in proteins: Comparison of dielectric and charge models. *Protein Eng.* 4:903–10
87. Meyer T, Hanson PI, Stryer L, Schulman H. 1992. Calmodulin trapping by

calcium-calmodulin-dependent protein kinase. *Science* 256:1199–2202
88. Monera OD, Shaw GS, Zhu B-Y, Sykes BD, Kay CM, et al. 1992. Role of interchain alpha-helical hydrophobic interactions in Ca^{2+} affinity, formation, and stability of a two-sitc domain in troponin C. *Protein Sci.* 1:945–55
89. Nakayama S, Moncrief ND, Kretsinger RH. 1992. Evolution of EF-hand calcium-modulated proteins. II. Domains of several subfamilies have diverse cvolutionary histories. *J. Mol. Evol.* 34:416–48
90. O'Neil KT, DeGrado WF. 1989. The interaction of calmodulin with fluorescent and photoactive model peptides: Evidence of a short interdomain separation. *Proteins: Struct. Funct. Gen.* 6:284–93
91. O'Neil KT, DeGrado WF. 1990. How calmodulin binds its targets: sequence independent recognition of amphiphilic alpha-helices. *Trends Biochem. Sci.* 15:59–64
92. Pascual-Ahuir J-L, Mehler EL, Weinstein H. 1991. Calmodulin structure and function: Implication of arginine residues in the compaction related to ligand binding. *Mol. Eng.* 1:231–47
93. Pascual-Ahuir JL, Silla E. 1990. GEPOL: An improved description of molecular surfaces. I. Building the spherical surface set. *J. Comput. Chem.* 11:1047–60
94. Persechini A, Kretsinger RH. 1988. Towards a model of the calmodulin-myosin light chain kinase complex: Implications for calmodulin function. *J. Cardiovasc. Pharmacol.* 12 (Suppl.5): S1–12
95. Persechini A, Kretsinger RH. 1988. The central helix of calmodulin functions as a flexible tether. *J. Biol. Chem.* 263:12175–78
96. Putkey JA, Ono T, VanBerkum MFA, Means AR. 1988. Functional significance of the central helix in calmodulin. *J. Biol. Chem.* 263:11242–49
97. Rao ST, Wu S, Satyshur KA, Ling K-Y, Kung C, et al. 1993. Structure of *Paramecium tetraurelia* calmodulin at 1.8Å resolution. *Protein Sci.* 2:436–47
98. Rao U, Teeter MM, Erickson-Viitanen S, DeGrado WF. 1992. Calmodulin binding to alpha1-purothionin: Solution binding and modeling of the complex. *Proteins: Struct. Funct. Gen.* 14:127–38
99. Schulman H. 1993. The multifunctional Ca^{2+}/calmodulin-dcpcndcnt protein kinase. *Curr. Opin. Cell Biol.* 5:247–53
100. Schulman H, Hanson PI, Meyer T. 1992. Decoding calcium signals by multifunctional CaM kinase. *Cell Calcium* 13:401–11
101. Seaton BA, Hcad JF, Engelman DM, Richards FM. 1985. Calcium-induced increase in the radius of gyration and maximum dimension of calmodulin measured by small-angle x-ray scattering. *Biochemistry* 24:6740–43
102. Shelling JG, Sykes BD. 1985. ^1H Nuclear magnetic resonance study of the two calcium-binding sites of porcine intestinal calcium-binding protein. *J. Biol. Chem.* 260:8342–47
103. Silla E, Tunon I, Pascual-Ahuir JL. 1991. GEPOL: An improved description of molecular surfaces. II. Computing the molecular area and volume. *J. Comput. Chem.* 12:1077–88
104. Skelton NJ, Kordel J, Forsen S, Chazin WJ. 1990. Comparative structural analysis of the calcium free and bound states of the calcium regulatory protein calbindin D9k. *J. Mol. Biol.* 213:593–98
105. Skelton NJ, Kordel J, Akke M, Chazin WJ. 1992. Nuclear magnetic resonance studies of the internal dynamics in apo, $(Cd^{2+})1$ and $(Ca^{2+})2$ calbindin D9k. *J. Mol. Biol.* 227:1100–17
106. Starovasnik MA, Davis TN, Klevit RE. 1993. Similarities and differences between yeast and vertebrate calmodulin: An examination of the calcium-binding and structural properties of calmodulin from the yeast *Saccharomyces cerevisiae*. *Biochemistry* 32:3261–70
107. Starovasnik MA, Su D-R, Beckingham K, Klevit RE. 1992. A series of point mutations reveal interactions between the calcium-binding sites of calmodulin. *Protein Sci.* 1:245–53
108. Strynadka NCJ, James MNG. 1988. Two trifluoperazine-binding sites on calmodulin predicted from comparative molecular modeling with troponin-C. *Proteins: Struct. Funct. Gen.* 3:1–17
109. Strynadka NCJ, James MNG. 1989. Crystal structures of the helix-loop-helix calcium-binding proteins. *Annu. Rev. Biochem.* 58:951–98
110. Strynadka NCJ, James MNG. 1991. Towards an understanding of the effect of calcium on protein structure and function. *Curr. Opin. Struct. Biol.* 1:905–14
111. Sussman F, Weinstein H. 1989. On the ion selectivity in Ca-binding proteins: The cyclo(-L-Pro-Gly)3 peptide as a model. *Proc. Natl. Acad. Sci. USA* 86:7880–84

112. Svensson B, Jonsson B, Woodward C. 1990. Electrostatic contribution to the binding of Ca^{2+} in calbindin mutants. *Biophys. Chem.* 38:179–83
113. Svensson B, Jonsson B, Thulin E. 1993. Binding of Ca^{2+} to calmodulin and its tryptic fragments: Theory and experiment. *Biochemistry* 32:2828–34
114. Szebenyi DME, Moffat K. 1986. The refined structure of vitamin D-dependent calcium-binding protein from bovine intestine. *J. Biol. Chem.* 261: 8761–77
115. Tanaka T, Hidaka H. 1980. Hydrophobic regions function in calmodulin-enzyme(s) interaction. *J. Biol. Chem.* 255:11078–80
116. Tanaka T, Hidaka H. 1981. Interaction of local anesthetics with calmodulin. *Biochem. Biophys. Res. Commun.* 101: 447–53
117. Tansey MG, Word RA, Hidaka H, Singer HA, Schworer CM, et al. 1992. Phosphorylation of myosin light chain kinase by the multifunctional calmodulin-dependent protein kinase II in smooth muscle cells. *J. Biol. Chem.* 267:12511–16
118. Teleman A, Drakenberg T, Forsen S. 1986. Kinetics of Ca^{2+} binding to calmodulin and its tryptic fragments studied by ^{43}Ca-NMR. *Biochim. Biophys. Acta* 873:204–13
119. Torok K, Lane AN, Martin SR, Janot J-M, Bayley PM. 1992. Effects of calcium binding on the internal dynamic properties of bovine brain calmodulin, studied by NMR and optical spectroscopy. *Biochemistry* 31:3452–62
120. Trewhella J, Liddle WK, Heidorn DB, Strynadka N. 1989. Calmodulin and troponin C structures studied by Fourier transform infrared spectroscopy: effects of Ca^{2+} and Mg^{2+} binding. *Biochemistry* 28:1294–301
121. van Gunsteren WF. 1988. The role of computer simulation techniques in protein engineering. *Protein Eng.* 1:5–13
122. van Gunsteren WF, Berendsen HJC, Hermans J, Hol WGJ, Postma JPM. 1983. Computer simulation of the dynamics of hydrated protein crystals and its comparison with x-ray data. *Proc. Natl. Acad. Sci. USA* 80:4315–19
123. van Gunsteren WF, Brunne RM, Mark AE, van Helden SP. 1992. Computer simulation of biomolecules: Comparison with experimental data. In *Molecular Aspects of Biotechnology: Computational Models and Theories,* ed. J Bertran, pp. 105–22. Dordrecht, The Netherlands: Kluwer
124. van Gunsteren WF, Weiner PK, eds. 1989. *Computer Simulation of Biomolecular Systems.* Leiden, The Netherlands: ESCOM. 224 pp.
125. Verhoeven AS, Shea MA. 1993. Ca^{2+}-induced domain interactions of calmodulin. *Biophys. J.* 64:A169 (Abstr.)
126. Vorherr T, Kessler O, Mark A, Carafoli E. 1992. Construction and molecular dynamics simulation of calmodulin in the extended and in a bent conformation. *Eur. J. Biochem.* 204:931–37
127. Vyas NK, Meenakshi NV, Quiocho FA. 1987. A novel calcium binding site in the galactose-binding protein of bacterial transport and chemotaxis. *Nature* 327:635–38
128. Wang C-LA. 1989. pH-dependent conformational changes of wheat germ calmodulin. *Biochemistry* 28:4816–20
129. Wang CA, Zhan Q, Tao T, Gergely J. 1987. pH-dependent structural transition in rabbit skeletal troponin C. *J. Biol. Chem.* 262:9636–40
130. Wang CK, Cheung HC. 1985. Energetics of the binding of calcium and troponin I to troponin C from rabbit skeletal muscle. *Biophys. J.* 48:727–39
131. Wang JH, Pallen C, Sharma RK, Adachi AM, Adachi K. 1985. The calmodulin regulatory system. *Curr. Topics Cell Regul.* 27:419–36
132. Warshel A, Chu ZT, Parson WW. 1989. Dispersed polaron simulation of electron transfer in photosynthetic reaction center. *Science* 246:112–16
133. Warshel A, Hwang JK, Aqvist J. 1992. Computer simulations of enzymatic reactions: Examination of linear free-energy relationships and quantum-mechanical corrections in the initial proton-transfer step of carbonic anhydrase. *Faraday Disc.* 93: In press
134. Warshel A, Sussman F, King G. 1986. Free-energy of charges in solvated proteins: Microscopic calculations using a reversible charging process. *Biochemistry* 25:8368–72
135. Weber PC, Lukas TJ, Craig TA, Wilson E, King MM, et al. 1989. Computational and site-specific mutagenesis analyses of the asymmetric charge distribution on calmodulin. *Proteins: Struct. Funct. Genet.* 6:70–85
136. Weinstein H, ed. 1986. *Computational Approaches to Enzyme Structure and Function.* Basel: Karger. 164 pp.
137. Weinstein H. 1992. Computational simulations of molecular structure, dynamics and signal transduction in biological systems: Mechanistic implications for ecological physical chemistry. In *Ecological Physical Chemistry,* ed. L

Bonati, U Cosentino, M Lasagni, G Moro, D Pitea, A Schiraldi, pp. 1–16. Amsterdam: Elsevier

138. Weinstein H, Mehler EL. 1992. Structural specificity in the engineering of biological function: Insights from the dynamics of calmodulin. See Ref. 123, pp. 153–73
139. Yazawa M, Vorherr T, James P, Carafoli E, Yagi K. 1992. Binding of calcium by calmodulin: influence of the calmodulin binding domain of the plasma membrane calcium pump. *Am. Chem. Soc.* 31:3171–76
140. Yoo SH. 1992. Identification of the Ca^{2+}-dependent calmodulin-binding region of chromogranin A. *Biochemistry* 31:6134–40